

# A Practical Framework of Key Performance Indicators for Multi-Robot Lunar and Planetary Field Tests

Julia Richter\*,<sup>1</sup>, David Oberacker\*,<sup>2,3</sup>, Gabriela Ligeza<sup>4,5</sup>, Valentin T. Bickel<sup>6</sup>, Philip Arm<sup>1</sup>, William Talbot<sup>1</sup>, Marvin Grosse Besselmann<sup>2</sup>, Florian Kehl<sup>7,8</sup>, Tristan Schnell<sup>2</sup>, Hendrik Kolvenbach<sup>1</sup>, Rüdiger Dillmann<sup>2</sup>, Arne Roennau<sup>2,3</sup>, and Marco Hutter<sup>1</sup>

**Abstract**— Robotic prospecting for critical resources on the Moon, such as ilmenite, rare earth elements, and water ice, requires robust exploration methods given the diverse terrain and harsh environmental conditions. Although numerous analog field trials address these goals, comparing their results remains challenging because of differences in robot platforms and experimental setups. These missions typically assess performance using selected, scenario-specific engineering metrics that fail to establish a clear link between field performance and science-driven objectives. In this paper, we address this gap by deriving a structured framework of Key Performance Indicators (KPIs) from three realistic multi-robot lunar scenarios reflecting scientific objectives and operational constraints. Our framework emphasizes scenario-dependent priorities in efficiency, robustness, and precision, and is explicitly designed for practical applicability in field deployments. We validated the framework in a multi-robot field test and found it practical and easy to apply for efficiency- and robustness-related KPIs, whereas precision-oriented KPIs require reliable ground-truth data that is not always feasible to obtain in outdoor analog environments. Overall, we propose this framework as a common evaluation standard enabling consistent, goal-oriented comparison of multi-robot field trials and supporting systematic development of robotic systems for future planetary exploration.

**Index Terms**— Multi-robot systems, Planetary exploration, Mission planning

## I. INTRODUCTION

As interest grows in supporting long-term, sustainable presence on the Moon, robotic resource prospecting is becoming an increasingly important research area. This pursuit is underscored by ESA's Space Resource Strategy [1], which aims to enable sustainable exploration by locating and characterizing lunar regions expected to contain resources, such as permanently shadowed regions and pyroclastic deposits. However, reaching and characterizing these locations and resources remains technically challenging. The lunar surface features a wide range of terrain types, from smooth mare

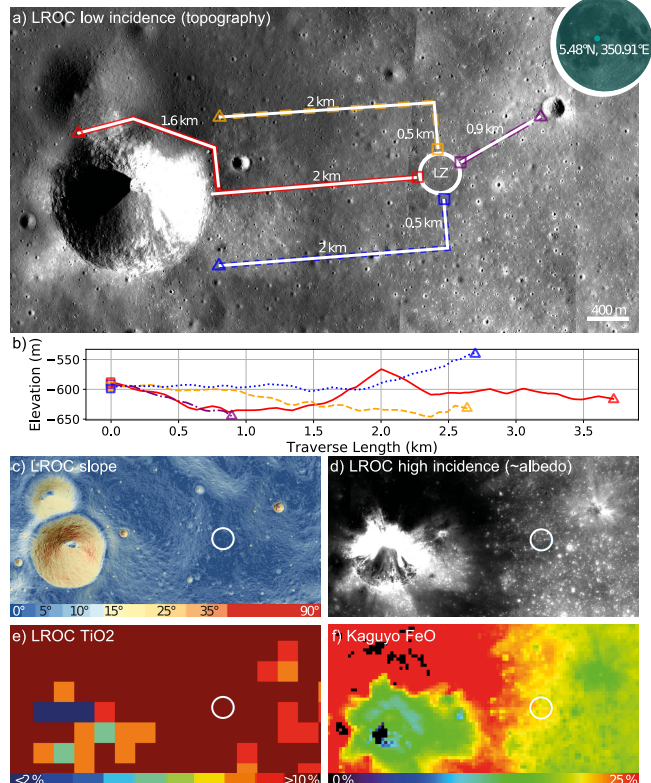


**Fig. 1:** Scenario 1 (Ilmenite). (a) LROC (Lunar Reconnaissance Orbiter) low-incidence image mosaic with landing zone (LZ), preliminary prospecting grid (white), and elevation transect (orange, red, blue, purple). (b) Elevation profile along the transect. (c–f) Selected orbital maps showcasing thermophysical, topographic, and compositional properties, with the LZ indicated by a white circle.

plains to steep crater walls and pits, each of which poses different requirements on robotic mobility, sensing capabilities, and autonomy.

Traditional approaches to planetary surface exploration typically rely on single robotic platforms, mostly wheeled rovers, such as Lunokhod 2, Yutu 2, Curiosity, or Perseverance. Although wheeled platforms perform well on flat terrain with minor obstacles, their performance is limited in more extreme terrain, such as unconsolidated regolith [2], steep slopes [3], and other unstructured environments. Recently, legged platforms have emerged as a viable alternative for traversing such terrains, as demonstrated for space analog environments [4,5]. However, this improved mobility

\* Equal contribution

<sup>1</sup> Robotic Systems Lab (RSL), ETH Zürich, Zürich, Switzerland

<sup>2</sup> FZI Research Center for Information Technology, Karlsruhe, Germany

<sup>3</sup> Machine Intelligence and Robotics Lab (MaiRo), Karlsruhe Institute for Technology (KIT), Karlsruhe, Germany

<sup>4</sup> Department of Environmental Sciences, University of Basel, Basel, Switzerland

<sup>5</sup> European Space Agency/ESTEC, Noordwijk, Netherlands

<sup>6</sup> Center for Space and Habitability, University of Bern, Switzerland

<sup>7</sup> Space Instruments Group, University of Zürich, Zürich, Switzerland

<sup>8</sup> Space Science and Technology, ETH Zürich, Zürich, Switzerland

Corresponding author: Julia Richter, [jurichter@ethz.ch](mailto:jurichter@ethz.ch).

comes at the cost of greater energy consumption, mechanical complexity, and control complexity, all of which increase the risk of failure.

Heterogeneous robotic teams that combine different locomotion and sensing capabilities can leverage both approaches to minimize this risk. Interest in such teams has been fueled by recent competitions, including the DARPA SubT [6] and the ESA-ESRIC Space Resources Challenge [7]. Despite imposing no restrictions on the architecture of the system, several teams in the Space Resources Challenge chose a heterogeneous, multi-robot solution [4,8,9]. This offered three main benefits: *redundancy*, in case of failure; *improved science acquisition rate* due to parallel operation; and *increased scientific depth* through specialised sensors.

Heterogeneous teams have also been used in analog missions such as the DLR ARCHES experiment on Mount Etna [10] and lava tube exploration for Martian cave analogs [11]. The plan for the NASA CADRE mission [12] aimed to flight-test a homogeneous swarm for cooperative lunar mapping.

Despite this progress, meaningful cross-comparison of multi-robot systems remains difficult. Most field experiments rely on a small set of scenario-specific metrics, often inherited from competition scoring rubrics. Existing KPI frameworks also focus on narrow subdomains, such as mapping or Human-Robot Interaction (HRI), and typically do not relate performance to scientific goals. Hence, there is a need for an easy-to-apply, comprehensive, and science-aligned KPI framework that enables cross-project comparison and thereby reveals weaknesses and opportunities for improvement.

In this study, we reverse the conventional approach of deriving KPIs from engineering field trials. Instead, we formulate metrics based on scientifically grounded operational scenarios co-developed by lunar geologists and roboticists, thereby ensuring both scientific relevance and operational measurability. We first outline three conceptual lunar missions targeting the prospecting of (i) ilmenite in volcanic plains, (ii) rare-earth-element-rich ejecta blankets, and (iii) polar water ice. We then extract a corresponding set of KPIs from these scenarios for evaluating heterogeneous multi-robot exploration strategies.

## II. RELATED WORK

### A. Lunar Mission Scenarios

Research on surface planetary exploration has proceeded along two largely independent tracks.

**Robotics-centric efforts** have consistently demonstrated that robots and robotic teams can autonomously explore lunar and Martian analog environments. Volcanoes [10,13], deserts [14], and lava tubes [11,15] are examples of such analog environments. In many of these studies, the primary focus lies on locomotion and mapping, whereas scientific objectives play a secondary role. Typical results are 3-dimensional maps [10,11,15] or collected samples [10,14]. The closest analog mission to a real planetary sampling scenario is the ARCHES Mount Etna campaign [10], in which pre-selected regions of interest from orbital imagery were first mapped and spectrally classified by an autonomous

rover-drone team, then revisited by a second rover that executed geochemical measurements and physical sample acquisition at the identified targets.

**Science-driven investigations**, such as ESA's Space Resources Strategy [1], have identified key lunar resources, including Rare Earth Element (REE), water ice, sunlight, Helium-3, and ilmenite. Drawing mainly from Lunar Reconnaissance Orbiter (LRO) [16] data, researchers have produced increasingly detailed, orbital-scale datasets that map these resources: radioactive materials, proxies for REE [17]; evidence for polar water ice [18]; estimates of regolith Helium-3 content [19]; and global  $\text{TiO}_2$  and  $\text{FeO}$  abundance maps [20], proxies for ilmenite. Landing site ranking frameworks translate this information into kilometer-scale regions of interest [21,22]. However, these frameworks rarely inform surface mission architectures; traverses, sampling strategies, and task allocations are rarely specified. Mission-level planning often occurs only after a flight opportunity has been formally identified. NASA's CADRE project is an example that combines autonomous multi-robot operations with a well-defined science case [12].

### B. Performance Analysis of Multi-Robot Missions

Multi-robot field trials are typically evaluated with competition scoring rubrics or subsystem KPIs, including *total mapped area* [4,8,14,23], *total distance traveled* [8,23,24,25], *map quality* [23,25], *exploration efficiency* [12] and *total planner-failure rates* [12]. The scientific value is measured based on the *rate of identified resources* [4,8,23,24,25] or the *rate of high-resolution images* [11]. Most field reports apply only a handful of scenario-specific engineering KPIs, making cross-team comparison difficult and leaving science-driven measures of knowledge gain largely unaddressed. Comparison frameworks for multi-robot exploration likewise restrict themselves to *map quality* [26,27,28], *exploration time* [26,29] and *exploration efficiency* [28,29], without links to science objectives.

In the HRI community, robotic field trials are evaluated with an emphasis on human factors. A survey of 29 studies [30] shows diverse HRI metrics, including various applicable metrics such as *time in unscheduled manual operations*, *task success*, and *number of interventions*. Others, however, are impractical in the field (e.g., estimating an operator's *degree of mental computation* or *human reliability*), qualitative (e.g., *robot self-awareness*), or setup-specific (e.g., *interaction effort* measured as camera-motion counts). Human workload is typically assessed by questionnaires [31], though recent work explores live psycho-physiological signals [32].

## III. MISSION SCENARIOS

Given that the primary motivation for lunar prospecting is resource identification, this section introduces three concrete mission scenarios centered on key lunar resources. Subsequently, robotic KPIs are designed to maximize the likelihood of success in these scenarios. We will first introduce a general mission design that is applicable to various prospecting missions. Subsequently, we propose concrete

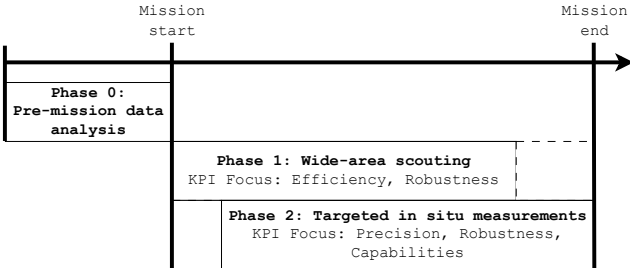


**Fig. 2:** General timeline of the mission concept, indicating relevant KPI focus for each phase.

mission scenarios based on the ESA Space Resource Strategy [1]. The selection of instruments for the missions proposed in this chapter is based on the work of Ligeza et al. [33].

#### A. Lunar Mission Design

We base all scenarios on a three-phase exploration strategy inspired by prior work, including the ARCHES campaign [10] and Team GLIMPSE [4] from the Space Resources Challenge [7], with a visual overview shown in Figure 2.

Before launch, **Phase 0** consists of analyzing orbital satellite data, e.g., LRO [16] accessible through the Lunar QuickMap [34], to obtain a coarse estimate of local resource abundances and define a preliminary prospecting grid.

Since in situ measurements are costly and time-consuming, this exploration strategy must be refined once the first agents reach the site. In **Phase 1** of each mission, scouting robots (*scouts*) map the prospecting area remotely (i.e., non-contact measurements) using optical and spectral cameras, tailored for the resource of interest. This data allows for refinement of the initial prospecting grid based on updated surface observations.

**Phase 2** follows with high-resolution, targeted in situ measurements by specialized robots (*scientists*). They conduct a systematic search at strategic locations and deploy scientific instruments for precise elemental analysis. Larger platforms can be equipped with specialized tools, such as robotic arms or drills, to deploy instruments and conduct subsurface measurements. Legged robots can access the interiors of craters, offering insight into the vertical distribution of resources. Depending on their mechanical configuration, they can utilize robotic arms or body-mounted instruments to conduct close-range tests in uneven terrain.

#### B. Scenario 1: Ilmenite Exploration

Ilmenite ( $FeTiO_3$ ) is a promising, quasi-globally abundant source of oxygen for life support and an oxidizer for propulsion [35]. While the horizontal extent of ilmenite can be inferred from its proxies  $TiO_2$  and  $FeO$ , the vertical extent is largely unknown [36]. The goal of this mission is therefore to (1) characterize vertical profiles using impact craters as natural windows into deeper layers, and (2) validate horizontal distributions with in situ measurements. The latter enables cross-correlation with orbital  $FeO$  and  $TiO_2$  maps, which is essential for validating remote-sensing techniques and extrapolating ilmenite abundance to unvisited locations.

We analyzed candidate lunar sites by starting from ilmenite-rich regions proposed by Gaddis et al. [37] and reviewing  $TiO_2/FeO$  maps in the Lunar QuickMap. We then selected the Sinus Aestuum region, which shows a clear, continuous gradient in both proxies (see Figure 1e,f). We defined a landing zone centered around  $5.48^\circ N$ ,  $350.91^\circ E$  based on the low slope ( $0.63^\circ$ ) and the low rock abundance (0.004), which gives the surface fraction covered by rocks larger than 1-2 m as defined by Powell et al. [38]. The approximately equatorial location of the site enables a mission lasting one lunar day ( $\sim 14$  Earth days). Measurements must be taken along the horizontal and vertical elemental gradient to meet scientific objectives. The area contains impact craters ranging from a few meters to approximately 1 km in diameter, enabling subsurface sampling at multiple depths, as the excavation depth scales with crater size according to impact mechanics [39]. Accessing these craters, however, requires traversing steep, rocky slopes of up to  $25^\circ$ .

This consideration leads to the following exploration strategy, which is also evident in the marked preliminary prospecting trajectory in Figure 1a. From the landing zone, scouts equipped with, e.g., spectral cameras rapidly assess the terrain to refine the exploration strategy for the scientists. Subsequently, scientists acquire detailed elemental compositions along the marked lines using Alpha Particle X-ray Spectrometers (APXSs), Lased-Induced Breakdown Spectrometers (LIBSs), or X-Ray Fluorescence Spectrometers (XRFs). Since these measurements require the robot to be stationary, we propose a 50 m sampling interval to match the resolution of the orbital  $FeO$  map.

#### C. Scenario 2: Rare Earth Element (REE) Exploration

REEs are valuable for various technologies on Earth, such as electronics, magnets, or batteries. Hence, the in situ supply of REE on the Moon could facilitate the construction and maintenance of those technologies for lunar infrastructure. They are concentrated in KREEP material, containing potassium (K), REE, and phosphorus (P), but also radioactive, heat-producing elements (e.g., thorium) that are detectable via remote sensing [17]. While these proxies can infer the approximate horizontal distribution of REE-bearing deposits, their vertical extent and internal nature remain poorly characterized, constraining assessments of accessibility and In Situ Resource Utilization (ISRU) potential [33].

Based on the orbital proxies, we identified several KREEP hotspots on the lunar nearside using Lunar QuickMap. Our chosen scenario targets a prominent site on the Aristarchus Plateau next to the Aristarchus crater, shown in Figure 3.

We define a landing zone centered around  $23.52^\circ N$ ,  $311.21^\circ E$  with a terrain slope of  $1.09^\circ$  and a rock abundance of 0.007. We propose an initial exploration strategy along the white lines in Figure 3a, sampling along the ejecta of the Aristarchus crater, as indicated by the rock abundance in Figure 3d. The terrain consists primarily of rocky ejecta, including densely packed boulder fields and smaller craters, with slope angles up to  $25^\circ$ . Line-of-sight communication with the lander may be hindered in areas of the ejecta blanket

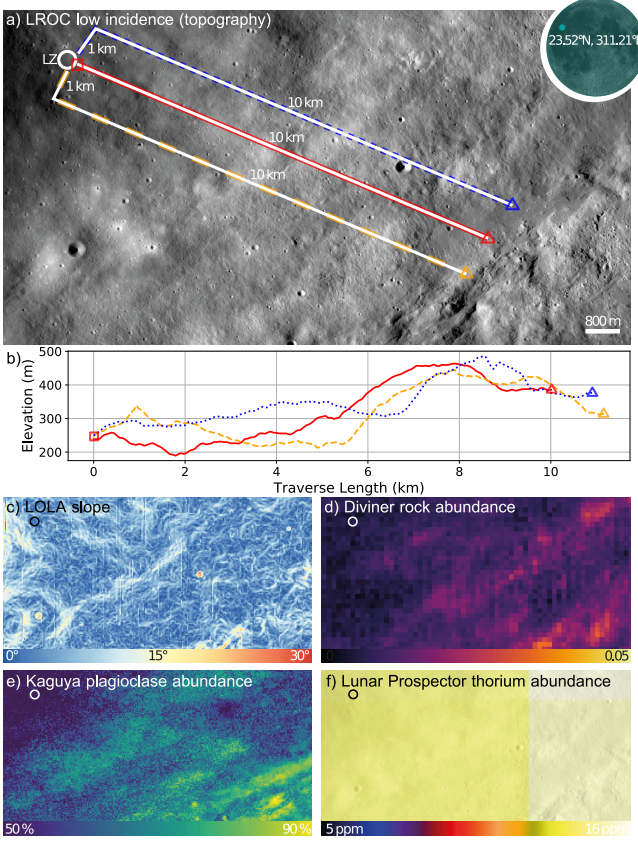


**Fig. 3:** Scenario 2 (KREEP). (a) LROC low-incidence image mosaic with landing zone (LZ), preliminary prospecting grid (white), and elevation transect (blue, red, orange). (b) Elevation profile along the transect. (c–f) Selected orbital maps showcasing thermophysical, topographic, and compositional properties, with the LZ indicated by a white circle.

where boulders and topographic undulations obstruct the signal. The equatorial location of the site enables a mission lasting one lunar day.

The scouts for this site are equipped with gamma-ray and neutron spectrometers, instruments that allow the remote detection of radioactive thorium and local KREEP hotspots [33]. Scientists then investigate these hotspots in situ using an XRF for elemental analysis and a laser-induced mass spectrometer for isotopic composition.

#### D. Scenario 3: Water Ice Characterization in Polar PSRs

Scenario 3 focuses on the characterization of water ice, a key resource for water supply for life support systems and hydrogen and oxygen for propellant production [35]. Surface-exposed water ice remains stable (over geologic time and under current lunar conditions) only below 110 K [18], concentrating deposits in Permanently Shadowed Regions (PSRs) near the lunar poles. The precise distribution, physical form, and abundance of lunar water ice are unknown [35]. Prospecting missions must not only detect water ice but also thoroughly characterize its thermophysical properties and the environmental conditions in which it occurs. These are essential for determining the feasibility of in situ extraction and its potential for processing.

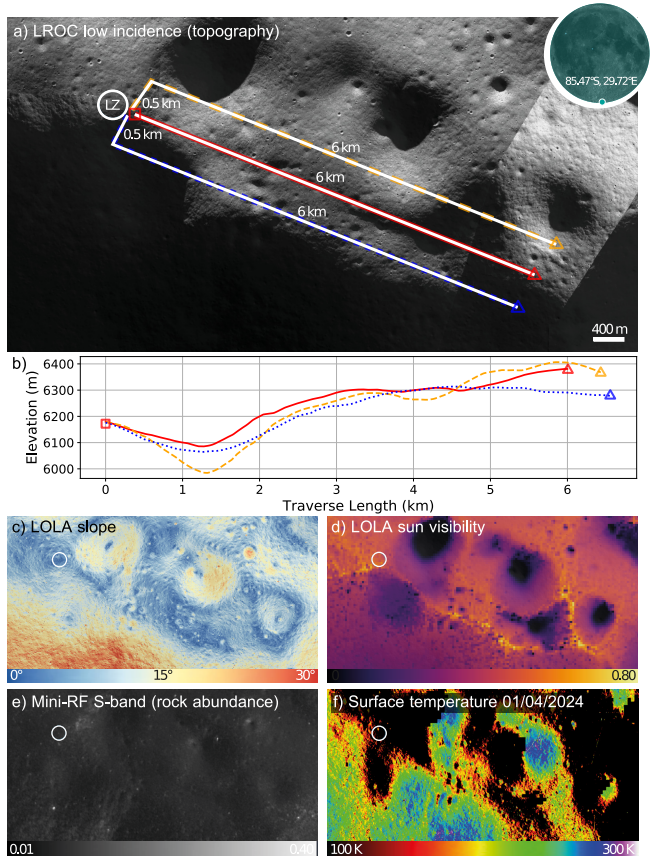


**Fig. 4:** Scenario 3 (Water ice). (a) LROC low-incidence image mosaic with landing zone (LZ), preliminary prospecting grid (white), and elevation transect (orange, red, blue). (b) Elevation profile along the transect. (c–f) Selected orbital maps showcasing thermophysical and topographic properties, with the LZ indicated by a white circle.

For this scenario, we adopt the same target region as NASA's previously planned VIPER mission [40]: the mountainous terrain west of the Nobile Crater, chosen for its relatively easy terrain and proximity to various PSRs. We define a landing zone centered around 85.47°S, 29.72°E with a mean slope of 1.24°. The rock abundance is unavailable for the polar regions, but Figure 4e shows a visual proxy. The mostly flat terrain includes varied PSR morphologies and predicted thermally stable zones (Figure 4f). Accessing specific PSRs may require traversing steep, locally rocky slopes, with slope angles up to 20°. Descents into craters and shadowed regions may require advanced communication planning between the lander and robotic assets. The geographic location leads to extreme temperature fluctuations, but enables a mission with a significantly extended duration, depending on the temperature resistance of the deployed lander and agents, as well as careful traverse planning [40].

The exploration strategy with the marked preliminary prospecting trajectory for this scenario is shown in Figure 4a. The scouts for this site are equipped with various remote sensing instruments, such as spectral cameras and neutron spectrometers, to aid in identifying potential water-bearing materials. Additional Ground Penetrating Radars (GPRs) penetrate beneath the lunar surface to provide information

**TABLE I:** Key Performance Indicators (KPIs) for Multi-Robot Lunar Missions.  $\downarrow$  = lower value is better,  $\uparrow$  = higher value is better.

Category	KPI	Unit	Definition
Efficiency	Mapping Efficiency $\uparrow$	$\text{m}^2 \text{ m}^{-1}$	Area mapped per meter traveled (total explored area / total distance traveled by all robots): $A_{\text{mapped}}/d_{\text{tot}}$
	Mapping Rate $\uparrow$	$\text{m}^2 \text{ s}^{-1}$	Area mapped per unit time (total explored area / mission time): $A_{\text{mapped}}/t_{\text{mission}}$
	Task Success Ratio $\uparrow$	%	Percentage of assigned tasks completed: $N_{\text{completed}}/N_{\text{total}} \times 100$
	Subjective Operator Workload $\downarrow$	–	Subjective operator workload assessed via standardized scales (e.g., NASA-TLX) or physiological proxies (e.g., pulse rate)
Robustness	Quantitative Operator Workload $\downarrow$	%	Percentage of mission time spent interacting with the robots: $t_{\text{operator}}/t_{\text{mission}} \times 100$
	Robot Downtime $\downarrow$	%	Percentage of mission time the robot cannot execute planned actions (e.g., waiting for commands or recovering from faults): $t_{\text{idle}}/t_{\text{mission}} \times 100$
	Autonomy Ratio $\uparrow$	–	Fraction of mission the robot operates without human intervention: $1 - \text{RAD}$ , with $\text{RAD} = t_{\text{IE}}/(t_{\text{IE}} + t_{\text{NT}})$ , where IE is the interaction effort and NT is the neglect tolerance
	Time in Unscheduled Manual Operations $\downarrow$	%	Percentage of mission time spent in unexpected teleoperation or manual override modes: $t_{\text{unscheduled-manual}}/t_{\text{mission}} \times 100$
	Retry Ratio $\downarrow$	%	Percentage of task attempts that were retries: $(N_{\text{attempts}} - N_{\text{success}})/N_{\text{attempts}} \times 100$
Precision	Science Acquisition Density $\uparrow$	$\text{m}^{-2}$	Number of valid scientific measurements per mapped area: $N_{\text{measurements}}/A_{\text{mapped}}$
	Science Acquisition Distribution $\uparrow$	–	Clark-Evans nearest-neighbor ratio $R$ of measurement locations ( $R=1$ random, $R<1$ clustered, $R>1$ dispersed)
	Localization Error $\downarrow$	m	Pose estimation error (e.g., RMSE of Absolute Trajectory Error for position)
	Instrument Placement Error $\downarrow$	m	Euclidean distance between commanded and achieved instrument locations (median or RMSE)
	Remote Sensing Error $\downarrow$	m	Euclidean distance between remotely sensed target and ground-truth measurements (e.g., RMSE over targets)
	Map Error $\downarrow$	m	Map-ground-truth discrepancy (e.g., bidirectional Chamfer distance): $d_{\text{Chamfer}}(M, GT)$
	Ratio of Identified Resources $\uparrow$	%	Percentage of ground-truth resources correctly detected: $N_{\text{resource}}/N_{\text{GT}} \times 100$

about subsurface water ice deposits. The scientists then investigate these targets *in situ* with LIBS for elemental identification and mass spectrometry for isotopic compositions.

#### IV. KPI DEFINITION

Lunar resource prospecting missions place four demands:

- 1) Cover a large area in a limited time,
- 2) Continue operation productively under unexpected or changing conditions,
- 3) Obtain and maximize scientific results.

To make these requirements measurable, we propose a KPI framework that maps each demand to a corresponding category: **Efficiency** (Req. 1), **Robustness** (Req. 2), and **Precision** (Req. 3). All formal definitions are provided in Table I.

**Efficiency** evaluates how well agents convert time, distance traveled, and operator attention to the mapped area and completed tasks, especially during scouting in *Phase I*. For *S1 (Ilmenite)* and *S2 (KREEP)*, broad areal coverage is essential to sample varying elemental concentrations along the gradient within the  $\sim 14$  day illumination window. While the total explored area is a primary mission outcome, it is typically dictated by the mission definition and therefore cannot be used to compare efficiency across different missions. Instead, we propose measuring *Mapping Efficiency* (area per meter travelled), and *Mapping Rate* (area per second). In order to calculate these values, the total area

$A_{\text{mapped}}$ , the total distance travelled  $d_{\text{tot}}$ , and the total mission duration  $t_{\text{mission}}$  are needed. All three quantities can be easily obtained by analysing the final created map and the recorded robot trajectories.

For *S3 (Water ice)*, the goal shifts from full coverage to successfully characterizing chosen PSRs. This requires completing high-risk tasks, such as crater descents and climb-outs, which are captured by the *Task Success Ratio*. To measure this value, task types must be clearly defined, and a consistent method for task logging must be implemented. While post-mission analysis of robot behavior is one option, we recommend explicit state logging that records when a task is assigned, when execution begins, and whether the robot successfully completes it.

Across all scenarios, human time is a scarce resource. High operator workload reduces scalability, increases error rates, and slows decision-making. Standardized questionnaires (e.g., NASA-TLX) and physiological proxies (e.g., pulse rate) can indicate *Subjective Operator Workload*, but they are either retrospective or strongly biased by the overall stress level typical for mission operations. We therefore complement these with a mission-integrated *Quantitative Operator Workload*, defined as the percentage of mission time humans spend operating the robots, which more directly reflects actual staffing needs during operations. To calculate this value, the total time the operator interacted with the robots,  $t_{\text{operator}}$ , must be measured along with the total

mission time,  $t_{mission}$ . This can be achieved either by implementing a logging system that detects operator-issued actions (e.g., teleoperation commands or button presses for task allocation) or by recording the operator and their screen and extracting interaction intervals through post-mission analysis.

**Robustness** evaluates how reliably the system maintains productive operation when conditions deviate from the plan, be it due to communication dropouts, unexpected terrain, or task failures. In *S2 (KREEP)*, long traverses ( $\sim 11$  km) make *Robot Downtime* a key limitation, as any idle period equates to lost coverage. It is measured as the percentage of mission time during which a robot did not contribute productively to mission progress, i.e., the ratio between its idle time  $t_{idle}$  (e.g., waiting for tasks or planning) and the total mission duration  $t_{mission}$ .

In *S3 (Water ice)*, the potential for fragile communication inside PSRs necessitates high autonomy. We quantify this with the *Autonomy Ratio*—defined as the inverse of Robot Attention Demand (RAD) [28]—and with *Time in Unscheduled Manual Operations*. The RAD is defined as

$$RAD = \frac{t_{IE}}{t_{IE} + t_{NT}} \quad (1)$$

where  $t_{IE}$  is the interaction effort, i.e., the time spent per operator interaction, and  $t_{NT}$  is the neglect tolerance, i.e., the time the robot remains productive without operator input. The *Time in Unscheduled Manual Operations* is defined as the percentage of mission time during which robots require unexpected teleoperation or manual override, measured as  $t_{unscheduled-manual}/t_{mission}$ . For evaluation of both metrics, explicit state logging—as introduced above—allows extraction of manual commands issued to the robots (e.g., teleoperation inputs) and the corresponding autonomous activities such as planning and execution.

Given the strict mission time budgets and the elevated risk of certain tasks, such as crater descents, robustness is further captured by the *Retry Ratio*, which quantifies the fraction of task attempts that were retries. This metric can be extracted directly from the same task logging mechanism.

**Precision** describes the scientific value of a mission by measuring the accuracy of locating, identifying, and quantifying resources. For *S1 (Ilmenite)* and *S2 (KREEP)*, which aim to map horizontal distributions, we emphasize taking “enough” and “well-spread” samples: *Science Acquisition Density* (samples per area) and *Science Acquisition Distribution*. For the latter, we propose using the Clark–Evans nearest-neighbor ratio  $R$  [41], which compares the observed mean nearest-neighbor distance to the value expected under a Poisson distribution representing complete spatial randomness. An  $R=1$  indicates a random pattern, and  $R<1$  clustering. We target  $R>1$ , corresponding to over-dispersion (i.e., a more uniform spacing than random). Both metrics can be computed directly from the logged measurement locations, requiring only the sample coordinates collected during the mission.

Accuracy in where and what we measure is equally critical. We therefore include *Localization Error* (robot pose),

*Instrument Placement Error* (where the tool touches down), and *Remote Sensing Error* (locating scientific targets by non-contact sensors, e.g., spectral cameras). Finally, accurate 3D terrain reconstructions from the scouting in *Phase 1* are essential for the science in *Phase 2*. Since path planning and coordination rely on map fidelity, we additionally include *Map Error*.

For *S2 (KREEP)* and *S3 (Water ice)*, where targeted resources are sparse, mission success depends on reliable detection and characterization. We therefore measure the *Ratio of Identified Resources*, which can be obtained in analog scenarios by comparing the set of detected resources against the known ground-truth resource locations.

## V. DISCUSSION

### A. Relevance of Proposed KPIs

The proposed KPI framework is designed to systematically evaluate the performance of heterogeneous robotic teams in relevant lunar prospecting scenarios. However, the relative importance of individual KPIs varies according to the specific objectives and constraints of each scenario. Accordingly, not all KPIs need to be reported for every field test; instead, experiments may select the subset that best aligns with their mission objectives and constraints. To illustrate this, we revisit the three scenarios introduced earlier and discuss which KPIs are most relevant for each scenario and mission phase, as summarized in Table II.

1) *Scalability of KPIs to Multi-Robot Teams*: While the proposed KPIs are motivated by multi-robot missions, many of them are not inherently tied to multi-robot coordination itself, but rather quantify general aspects of mission performance. Nevertheless, all KPIs are defined at the team level and can be directly applied to heterogeneous multi-robot systems by aggregating robot-level measurements and relating them to shared mission objectives. In this way, the framework remains applicable to both single- and multi-robot deployments, while explicitly capturing the benefits and challenges that emerge when multiple robots operate in parallel.

2) *Efficiency*: These KPIs capture the effectiveness of resource utilization in exploration. For *S1 (Ilmenite)* and *S2 (KREEP)*, dense and rapid mapping (E.1, E.2) is essential, especially for the scouting phase. In contrast, *S3 (Water ice)* prioritizes detailed characterization within selected PSRs rather than extensive area coverage, making broad area efficiency less critical.

3) *Robustness*: Robustness KPIs quantify how reliably robotic systems operate under challenging conditions. In *S2*, where long traverses are necessary, minimizing *Robot Downtime* (R.1) is crucial. *S2* and *S3*, which involve unstable or limited communication, require higher autonomy, making *Autonomy Ratio* (R.2) and *Time in Unscheduled Manual Operations* (R.3) key indicators of operational robustness.

4) *Precision*: Precision KPIs directly link to scientific quality, emphasizing accurate identification, localization, and quantification of lunar resources. The *Ratio of Identified Resources* (P.7) is particularly relevant for *S2* and *S3*, where

**TABLE II:** Relevance of each KPI for scenario–phase combinations. Phase 1 (p1) refers to wide-area scouting, Phase 2 (p2) to targeted in situ operations. KPIs are classified in: ● highly relevant; ● relevant; ○ not relevant.

KPI	S1		S2		S3	
	p1	p2	p1	p2	p1	p2
E.1 Mapping Efficiency	●	○	●	○	○	○
E.2 Mapping Rate	●	○	●	○	○	○
E.3 Task Success Ratio	●	●	●	●	●	●
E.4 Subjective Operator Workload	●	●	●	●	●	●
E.5 Quantitative Operator Workload	●	●	●	●	●	●
R.1 Robot Downtime	○	○	●	●	○	○
R.2 Autonomy Ratio	○	○	●	●	●	●
R.3 Time in Unscheduled Manual Ops	○	○	●	●	●	●
R.4 Retry Ratio	●	●	●	●	●	●
P.1 Science Acquisition Density	○	●	○	○	●	●
P.2 Science Acquisition Distribution	○	●	○	○	●	●
P.3 Localization Error	●	●	○	○	●	●
P.4 Instrument Placement Error	○	●	○	●	○	●
P.5 Remote Sensing Error	●	●	●	●	●	●
P.6 Map Error	●	●	○	○	●	●
P.7 Ratio of Identified Resources	○	○	○	●	●	●

targeted resources are sparse, requiring reliable detection and characterization. Conversely, S1 emphasizes correlating in situ data with orbital measurements, making the measurement distribution (P.1, P.2) and localization metrics (P.3, P.6) more significant.

### B. Advantages of Scenario-Based KPI Development

Grounding KPI selection in realistic mission scenarios highlights the practical value of each metric compared to previous frameworks. Traditional metrics, such as *Total Distance Traveled*, offer limited insights unless directly linked to scientific outcomes, making *Mapping Efficiency* a more meaningful comparative measure.

Previous studies often prioritized *Task Success Ratio*, but this framework also emphasizes *Retry Ratio* to capture inefficiencies arising from task repetition specifically. Metrics such as *Ratio of Identified Resources*, crucial in resource-sparse contexts, are scenario-dependent and may not universally reflect mission success, exemplified by S1 (*Ilmenite*).

In contrast, previously omitted metrics, such as *Instrument Placement Error* and *Remote Sensing Error*, reflect the reliability and scientific relevance of the gathered data, thereby providing valuable insights. Furthermore, traditional terrestrial metrics such as *Robot Downtime* need to be redefined in lunar contexts, where strategic downtime (e.g., thermal management, solar charging) may be deliberate and beneficial rather than inefficient.

### C. Feasibility and Practicality of KPI Measurement

Ensuring that KPIs can be practically measured in terrestrial field tests is crucial for their applicability and was thus a main objective of this work. We therefore evaluated the feasibility of KPI extraction in a multi-robot field deployment, which implemented a lunar-analog prospecting sce-



**Fig. 5:** Heterogeneous robotic team during the lunar-analog field deployment used to assess the practical applicability of the proposed KPI framework.

nario focused on detecting and mapping discrete boulders and soil patches. The team consisted of one operator and five robots: three scouts and two scientists. In contrast to the here introduced scenarios, where broad areal mapping and spatial coverage are primary objectives, our field trial emphasized reliably finding and confirming sparse resources, making it most comparable to S2 (*KREEP*) in terms of search and verification behavior. Details of the deployment, methodology, and the resulting KPI values are reported in the corresponding paper [42]. Here, we focus on assessing the practicality of applying the proposed KPI framework in a real-world setting.

Overall, the time- and activity-based **Robustness** metrics (*Robot Downtime*, *Autonomy Ratio*, *Time in Unscheduled Manual Operations*, and *Retry Ratio*) can be extracted reliably when the mission software provides explicit state logging for task assignment, execution, and completion, as well as for manual interventions. In our deployment, we used a behavior-tree-based control system that tracked task assignment and execution, enabling the reconstruction of a detailed timeline of each robot’s activities. As a result, all timestamps required to compute these KPIs were available.

Operator workload metrics require more careful integration into the mission setup. While *Subjective Operator Workload* is inherently difficult to assess objectively in field conditions—since field tests are generally stressful and exhausting, particularly when the operator is part of the development team—we decided against using this measure and instead focused on *Quantitative Operator Workload*. Although this metric is in principle measurable, it is non-trivial to implement robustly. In our field test, we ultimately estimated it through post-mission video annotation of the operator and screen recordings, which proved feasible but noisy. We therefore recommend implementing dedicated logging of operator-issued actions (e.g., teleoperation commands, task dispatches, and autonomy mode overrides) to directly compute interaction time. In particular, automatically capturing interactions performed through RViz can be challenging, as they may correspond to diverse UI actions that

do not consistently map to a single logged robot command. The remaining **Efficiency** KPIs, namely *Mapping Efficiency*, *Mapping Rate*, and *Task Success Ratio*, were comparatively easy to measure based on the produced 3D map, the recorded traversal distances of the robots, and manually annotated task success.

*Science Acquisition Density* and *Science Acquisition Distribution* were not evaluated in our field trial, as the mission objective focused on resource identification rather than dense sampling for spatial distribution mapping, rendering these **Precision** KPIs irrelevant in this context. Moreover, the metrics *Localization Error*, *Instrument Placement Error*, and *Remote Sensing Error* rely on accurate ground-truth data (e.g., surveyed target locations or reference maps), which were not available for our deployment. In contrast, the *Ratio of Identified Resources* can be readily evaluated as long as the number and approximate locations of the ground-truth resources are known.

In summary, the proposed KPI framework proved easy to apply for **Efficiency** and **Robustness** metrics, provided that the mission software includes sufficiently detailed state and interaction logging. Most time- and activity-based KPIs can be extracted directly from such logs with minimal additional instrumentation. In contrast, **Precision** metrics require substantially more preparation, as they depend on the availability of reliable ground-truth data, such as surveyed maps or reference target locations, which is not always feasible in outdoor analog field tests. This highlights the importance of aligning the selected KPIs with both the mission objectives and the practical constraints of the experimental setup.

#### D. Limitations and KPI Trade-offs

Several proposed KPIs are correlated, which may require thoughtful interpretation during analysis. For instance, *Mapping Efficiency*, *Total Explored Area*, and *Total Distance Traveled* all relate to coverage; however, *Mapping Efficiency* provides the most meaningful basis for cross-comparison between different missions. Similarly, while *Subjective* and *Quantitative Operator Workload* assess operator burden, subjective assessments may be more insightful but more complex to measure consistently.

Metrics such as *Retry Ratio* and *Task Success Ratio* reflect task reliability. Still, the former emphasizes inefficiency caused by task repetition, while the latter focuses on the ultimate completion of the task.

Trade-offs between KPIs must also be explicitly considered in mission design. Optimizing *Science Acquisition Density* typically lowers *Explored Area*, and high *Mapping Rates* may compromise precision (e.g., *Map Error* or *Ratio of Identified Resources*).

Thus, selecting optimal KPI targets must be done with respect to the specific context of the scenario, taking into account scientific priorities, terrain conditions, and available resources. This ensures system performance is evaluated meaningfully while acknowledging the trade-offs between efficiency, robustness, and data quality in real mission scenarios.

## VI. CONCLUSION

This paper addresses the challenge of robotic resource prospecting in extraterrestrial environments by introducing three representative lunar mission scenarios targeting ilmenite, rare-earth elements, and water ice. Based on these scenarios, we propose a structured KPI framework that systematically evaluates the performance of heterogeneous robotic teams while explicitly accounting for scenario-specific objectives and operational constraints. As a result, the relative importance of individual KPIs naturally varies across scenarios and mission phases, reflecting different scientific goals and risk profiles.

We validated the proposed framework in a real multi-robot field deployment and found it straightforward to apply to efficiency- and robustness-related KPIs, provided that appropriate mission-state and interaction logging is available. In contrast, precision-oriented KPIs require additional preparation, such as reliable ground-truth data, which is not always feasible in outdoor analog environments. While most KPIs quantify general mission performance rather than explicit inter-robot coordination, they are defined at the team level and naturally extend to heterogeneous multi-robot systems through aggregation and shared mission objectives. Overall, the framework provides a clear and practical basis for evaluating heterogeneous robotic teams, enabling meaningful cross-mission comparisons, informed mission design, and targeted technological development for future lunar exploration.

## ACKNOWLEDGMENT

This work was supported by the European Space Agency (ESA) (Ref. 4000141520/23/NL/AT), the Luxembourg National Research Fund (Ref. 18990533), and the Swiss National Science Foundation (SNSF) as part of the projects No.200021E\_229503 and No.227617.

## REFERENCES

- [1] European Space Agency, “Esa space resources strategy,” European Space Agency, Paris, France, Technical Report, May 2019, covers period up to 2030; last updated September 1, 2019. [Online]. Available: <https://exploration.esa.int/web/moon/-/61369-esa-space-resources-strategy>
- [2] L. David. (2005) Opportunity mars rover stuck in sand. Accessed: 2025-07-18. [Online]. Available: <https://www.space.com/1019-opportunity-mars-rover-stuck-sand.html>
- [3] N. J. Potts, A. L. Gullikson, N. M. Curran, J. K. Dhaliwal, M. K. Leader, R. N. Rege, K. K. Klaus, and D. A. Kring, “Robotic traverse and sample return strategies for a lunar farside mission to the schrödinger basin,” *Advances in Space Research*, vol. 55, no. 4, pp. 1241–1254, 2015.
- [4] P. Arm, G. Waibel, J. Preisig, T. Tuna, R. Zhou, V. Bickel, G. Ligeza, T. Miki, F. Kehl, H. Kolvenbach *et al.*, “Scientific exploration of challenging planetary analog environments with a team of legged robots,” *Science robotics*, vol. 8, no. 80, p. eade9548, 2023.
- [5] H. Kolvenbach, P. Arm, E. Hampp, A. Dietsche, V. Bickel, B. Sun, C. Meyer, and M. Hutter, “Traversing steep and granular martian analog slopes with a dynamic quadrupedal robot,” *Field robotics*, vol. 2, pp. 910–939, 2022.
- [6] U.S. Department of Defense, “Subterranean challenge,” <https://www.defense.gov/Multimedia/Experience/Subterranean-Challenge/>, 2021, accessed: 2025-07-18.
- [7] European Space Agency, “The challenge 2021–2022,” <https://src.esa.int/the-challenge-2021-2022/>, 2023, accessed: 2025-07-18.

[8] T. Schnell, D. Oberacker, F. Exner, L. Puck, M. G. Besselmann, N. Spielbauer, C. Plasberg, A. Roennau, and R. Dillmann, "An efficient scalable autonomy approach for teams of heterogeneous mobile robots," in *2023 IEEE 19th International Conference on Automation Science and Engineering (CASE)*. IEEE, 2023, pp. 1–7.

[9] Space Applications Services. (2022) LUVMI-XR Team Passes First Field Trial of the Space Resources Challenge. Accessed: 2025-07-18. [Online]. Available: <https://www.spaceapplications.com/news/luvmi-xr-team-passes-first-field-trial-of-the-space-resources-challenge>

[10] M. J. Schuster, M. G. Müller, S. G. Brunner, H. Lehner, P. Lehner, R. Sakagami, A. Dömel, L. Meyer, B. Vodermayer, R. Giubilato *et al.*, "The arches space-analogue demonstration mission: Towards heterogeneous teams of autonomous robots for collaborative scientific sampling in planetary exploration," *IEEE Robotics and Automation Letters*, vol. 5, no. 4, pp. 5315–5322, 2020.

[11] B. J. Morrell, M. S. da Silva, M. Kaufmann, S. Moon, T. Kim, X. Lei, C. Patterson, J. Uribe, T. S. Vaquero, G. J. Correa *et al.*, "Robotic exploration of martian caves: Evaluating operational concepts through analog experiments in lava tubes," *Acta Astronautica*, vol. 223, pp. 741–758, 2024.

[12] S. Nayak, G. Lim, F. Rossi, M. Otte, and J.-P. de la Croix, "Multi-robot exploration for the cadre mission," *Autonomous Robots*, vol. 49, no. 2, p. 17, 2025.

[13] L. Burkhard, R. Sakagami, K. Lakatos, H. Gmeiner, P. Lehner, J. Reill, M. G. Müller, M. Durner, and A. Wedler, "Collaborative multi-rover crater exploration: Concept and results from the arches analog mission," in *2024 IEEE Aerospace Conference*. IEEE, 2024, pp. 1–14.

[14] R. Sonsalla, F. Cordes, L. Christensen, T. M. Roehr, T. Stark, S. Planthaber, M. Maurus, M. Mallwitz, and E. A. Kirchner, "Field testing of a cooperative multi-robot sample return mission in mars analogue environment," in *Proceedings of the 14th symposium on advanced space technologies in robotics and automation (ASTRA)*, 2017.

[15] W. Brinkmann, L. Danter, A. Suresh, M. Yüksel, M. Meder, and F. Kirchner, "Development strategies for multi-robot teams in context of planetary exploration," in *2024 International Conference on Space Robotics (iSpaRo)*. IEEE, 2024, pp. 64–69.

[16] NASA Science. (2025) Lunar Reconnaissance Orbiter. National Aeronautics and Space Administration. Page last updated 1 July 2025. Accessed 21 July 2025. [Online]. Available: <https://science.nasa.gov/mission/lro/>

[17] M. Anand, I. A. Crawford, M. Balat-Pichelin, S. Abanades, W. Van Westrenen, G. Péraudeau, R. Jaumann, and W. Seboldt, "A brief review of chemical and mineralogical resources on the moon and likely initial in situ resource utilization (isru) applications," *Planetary and Space Science*, vol. 74, no. 1, pp. 42–48, 2012.

[18] P. O. Hayne, A. Hendrix, E. Sefton-Nash, M. A. Siegler, P. G. Lucey, K. D. Retherford, J.-P. Williams, B. T. Greenhagen, and D. A. Paige, "Evidence for exposed water ice in the moon's south polar regions from lunar reconnaissance orbiter ultraviolet albedo and temperature measurements," *Icarus*, vol. 255, pp. 58–69, 2015.

[19] W. Fa and Y.-Q. Jin, "Quantitative estimation of helium-3 spatial distribution in the lunar regolith layer," *Icarus*, vol. 190, no. 1, pp. 15–23, 2007.

[20] H. Sato, M. S. Robinson, S. J. Lawrence, B. W. Denevi, B. Hapke, B. L. Jolliff, and H. Hiesinger, "Lunar mare tio2 abundances estimated from uv/vis reflectance," *Icarus*, vol. 296, pp. 216–238, 2017.

[21] J. Liu, X. Zeng, C. Li, X. Ren, W. Yan, X. Tan, X. Zhang, W. Chen, W. Zuo, Y. Liu *et al.*, "Landing site selection and overview of china's lunar landing missions," *Space science reviews*, vol. 217, no. 1, p. 6, 2021.

[22] S. Kim, K. J. Kim, and Y. Yi, "Investigation on lunar landing candidate sites for a future lunar exploration mission," *International Journal of Aeronautical and Space Sciences*, vol. 23, no. 1, pp. 221–232, 2022.

[23] A. Agha, K. Otsu, B. Morrell, D. D. Fan, R. Thakker, A. Santamaría-Navarro, S.-K. Kim, A. Bouman, X. Lei, J. Edlund *et al.*, "Nebula: Quest for robotic autonomy in challenging environments; team costar at the darpa subterranean challenge," *arXiv preprint arXiv:2103.11470*, 2021.

[24] R. Sakagami, S. G. Brunner, A. Dömel, A. Wedler, and F. Stulp, "Rosmc: A high-level mission operation framework for heterogeneous robotic teams," in *2023 IEEE International Conference on Robotics and Automation (ICRA)*. IEEE, 2023, pp. 5473–5479.

[25] N. Hudson, F. Talbot, M. Cox, J. Williams, T. Hines, A. Pitt, B. Wood, D. Froushiger, K. L. Surdo, T. Molnar *et al.*, "Heterogeneous ground and air platforms, homogeneous sensing: Team csiro data61's approach to the darpa subterranean challenge," *Field Robotics*, vol. 2, pp. 595–636, 2022.

[26] Z. Yan, L. Fabresse, J. Laval, and N. Bouraqadi, "Metrics for performance benchmarking of multi-robot exploration," in *2015 IEEE/RSJ International Conference on Intelligent Robots and Systems (IROS)*. IEEE, 2015, pp. 3407–3414.

[27] B. Balaguer, S. Balakirsky, S. Carpin, and A. Visser, "Evaluating maps produced by urban search and rescue robots: lessons learned from robocup," *Autonomous Robots*, vol. 27, no. 4, pp. 449–464, 2009.

[28] P. Arm, H. Kolvenbach, and M. Hutter, "Comparison of legged single-robot and multi-robot planetary analog exploration systems," in *IAC 2023 Conference Proceedings*. International Astronautical Federation, 2023, p. 78381.

[29] Y. Xu, J. Yu, J. Tang, J. Qiu, J. Wang, Y. Shen, Y. Wang, and H. Yang, "Explore-bench: Data sets, metrics and evaluations for frontier-based and deep-reinforcement-learning-based autonomous exploration," in *2022 International Conference on Robotics and Automation (ICRA)*. IEEE, 2022, pp. 6225–6231.

[30] R. R. Murphy and D. Schreckenghost, "Survey of metrics for human-robot interaction," in *2013 8th ACM/IEEE International Conference on Human-Robot Interaction (HRI)*. IEEE, 2013, pp. 197–198.

[31] S. G. Hart and L. E. Staveland, "Development of nasa-tlx (task load index): Results of empirical and theoretical research," in *Advances in psychology*. Elsevier, 1988, vol. 52, pp. 139–183.

[32] J. Nelles, S. T. Kwee-Meier, and A. Mertens, "Evaluation metrics regarding human well-being and system performance in human-robot interaction—a literature review," in *Congress of the International Ergonomics Association*. Springer, 2019, pp. 124–135.

[33] G. Ligeza, V. T. Bickel, I. Drozdovskiy, T. Bontognali, N. Kuhn, and F. Kehl, "Exploring the lunar surface: A review of technologies for resource prospection and their complementarity," *Acta Astronautica*, 2025, under review.

[34] LROC Science Operations Center. (2025) ACT–REACT QuickMap — Lunar Reconnaissance Orbiter Camera. NASA/GSFC & Arizona State University. Accessed 21 July 2025. [Online]. Available: <https://quickmap.lroc.asu.edu/>

[35] I. A. Crawford, "Lunar resources: A review," *Progress in Physical Geography*, vol. 39, no. 2, pp. 137–167, 2015.

[36] T. A. Giguere, B. R. Hawke, J. J. Gillis-Davis, M. Lemelin, J. M. Boyce, D. Trang, S. J. Lawrence, J. D. Stopar, B. A. Campbell, L. R. Gaddis *et al.*, "Volcanic processes in the gassendi region of the moon," *Journal of Geophysical Research: Planets*, vol. 125, no. 9, p. e2019JE006034, 2020.

[37] L. R. Gaddis, M. I. Staid, J. A. Tyburczy, B. R. Hawke, and N. E. Petro, "Compositional analyses of lunar pyroclastic deposits," *Icarus*, vol. 161, no. 2, pp. 262–280, 2003.

[38] T. Powell, T. Horvath, V. L. Robles, J.-P. Williams, P. Hayne, C. Gallinger, B. Greenhagen, D. McDougall, and D. Paige, "High-resolution nighttime temperature and rock abundance mapping of the moon using the diviner lunar radiometer experiment with a model for topographic removal," *Journal of Geophysical Research: Planets*, vol. 128, no. 2, p. e2022JE007532, 2023.

[39] J. D. Stopar, M. S. Robinson, O. S. Barnouin, A. S. McEwen, E. J. Speyerer, M. R. Henriksen, and S. S. Sutton, "Relative depths of simple craters and the nature of the lunar regolith," *Icarus*, vol. 298, pp. 34–48, 2017.

[40] A. Colaprete, "Volatiles investigating polar exploration rover (viper) proposal information package," NASA, Tech. Rep., 2021. [Online]. Available: <https://science.nasa.gov/wp-content/uploads/2024/08/viper-pip-final.pdf>

[41] P. J. Clark and F. C. Evans, "Distance to nearest neighbor as a measure of spatial relationships in populations," *Ecology*, vol. 35, no. 4, pp. 445–453, 1954.

[42] D. Oberacker, J. Richter, P. Arm, M. Grosse Besselmann, L. Puck, W. Talbot, M. Schik, S. Bellmann, T. Schnell, H. Kolvenbach, R. Dillmann, M. Hutter, and A. Roennau, "MOSAIC: Modular scalable autonomy for intelligent coordination of heterogeneous robotic teams," 2026, manuscript under review.